Available online at www.sciencedirect.com
ScienceDirect
European Polymer Journal 44 (2008) 608–614
EUROPEAN POLYMER JOURNAL
www.elsevier.com/locate/europolj

Macromolecular Nanotechnology

Performance of gelled-type dye-sensitized solar cells associated with glass transition temperature of the gelatinizing polymers

Chi-Wei Tu [a], Ken-Yen Liu [b], An-Ting Chien [a], Chia-Hsin Lee [b], Kuo-Chuan Ho [a], King-Fu Lin [a,b,*]

[a] *Institute of Polymer Science and Engineering, National Taiwan University, Taipei, Taiwan, ROC*
[b] *Department of Materials Science and Engineering, National Taiwan University, No. 1, Roosevelt Road, Section 4, Taipei, Taiwan, ROC*

Received 12 September 2007; received in revised form 19 December 2007; accepted 4 January 2008
Available online 12 January 2008

Abstract

Poly(methyl acrylate) (PMA), poly(vinyl acetate) (PVAc) and poly(*n*-isopropylacrylamide) (PNIPAAm) with their respective T_g of 6, 32, and 145 °C were employed to gel the LiI/I_2/tertiary butylpyridine electrolyte system for preparation of the gelled-type dye-sensitized solar cells (DSSC). The light-to-electricity conversion efficiencies of DSSCs gelled by PMA, PVAc, and PNIPAAm were 7.17%, 5.62%, and 3.17%, respectively under simulated AM 1.5 sunlight irradiation, implying that utilizing the polymer of lower T_g to gel the electrolytes leaded to better performance of the DSSCs. Their short-circuit current density and IPCE also showed the similar trend. Electrochemical impedance spectroscopy of the gelled DSSCs revealed that utilizing the polymer of lower T_g resulted in lower impedance associated with the Nernstian diffusion within the electrolytes. The results were consistent with the observation that the molar conductivity of gelled electrolytes was higher as the polymer of lower T_g was applied, which can be justified by Vogel–Tammann–Fulcher (VTF) equation.

Keywords: Dye-sensitized solar cell; Glass transition temperature; Conductivity; Gel; Photovoltaic

1. Introduction

Dye-sensitized solar cells (DSSCs) based on a monolayer of ruthenium dye adsorbing onto the nanocrystalline TiO_2 layer have attracted significant interest in past years, because of their high energy conversion efficiency (η) and low production cost [1–4]. Notably, $\eta \geqslant 11\%$ has been achieved in the liquid-type DSSC sensitized with *cis*-di(thiocyanato)-bis(2,2′-bipyridyl-4,4′-dicarboxylate)ruthenium(II) dye. Basically, the sun light excites the dye to generate the excited electrons, which then inject into the conduction band of TiO_2. The resulting oxidized dye needs immediately reduced by the redox couples

* Corresponding author. Address: Department of Materials Science and Engineering, National Taiwan University, No. 1, Roosevelt Road, Section 4, Taipei, Taiwan, ROC. Tel.: +886 2 3366 1315; fax: +886 2 2363 4562.
E-mail address: kflin@ccms.ntu.edu.tw (K.-F. Lin).

0014-3057/$ - see front matter © 2008 Elsevier Ltd. All rights reserved.
doi:10.1016/j.eurpolymj.2008.01.005

such as I^-/I_3^- in solution before charge recombination. The oxidized redox couples were then reduced in the counter electrode [5]. Thus, the electrolyte system for charge separation and transportation plays an important role to determine the photovoltaic efficiency. Liquid solvents such as acetonitrile have been normally employed for dissolving the redox couples. However, they have problems of leakage and evaporation [6–8].

Poly(ethylene oxide) (PEO)-based polymers, copolymers and polyblends have been frequently used to gel the electrolyte systems for the preparation of polymer-gelled DSSCs [9–17]. However, owing to the tendency of crystallization of PEO segments that is detrimental to the ionic conductivity of electrolytes [15], the reported energy conversion efficiency (η) of prepared gelled-type DSSCs was never over 4%. Other polymers that were used to gel the electrolyte systems for the preparation of gelled DSSCs showed scattered results [18–23]. For example, the DSSC using poly(acrylonitrile) to gel the electrolytes had $\eta = 2.67\%$ [18], whereas that using poly(vinylidenefluoride-co-hexafluoropropylene) had $\eta > 6\%$ [23]. However, so far there still has no systematic study to predict what type of the polymer to gel the electrolyte system can obtain better efficiency.

Notably, it has been suggested that photocurrent (J_{ph}) of the DSSCs is linearly proportional to the diffusion coefficient of oxidized redox couples in the solution [24]

$$J_{ph} = -zFD\frac{dc_{ox}(x)}{dx} \quad (1)$$

where $c_{ox}(x)$ is the concentration of oxidized redox couples in solution at location x between the fluorine-doped tin oxide (FTO)/TiO_2 interface and the counter electrode, z is the number of electrons transferred from TiO_2 to an oxidized redox couple, D is the diffusion coefficient of the oxidized redox couples, and F is the Faraday constant. In addition, ionic conductivity (σ) of the electrolytes including the oxidized redox couples is related to their diffusion coefficients by [23]

$$\sigma(T) = \sum_i \frac{|z_i|^2 F c_i e D_i}{K_B T} \quad (2)$$

where z_i, c_i, and D_i are the charge, concentration and diffusion coefficient of the ith ion, e is the electronic charge, T is the absolute temperature and K_B is the Boltzmann constant. Grätzel et al. [23] have pointed out that the conductivity–temperature data of polymer-gelled electrolytes were better fit by the Vogel–Tammann–Fulcher (VTF) equation [25].

$$\sigma(T) = AT^{-1/2}\exp[-B/(T - T_0)] \quad (3)$$

where A and B are constants and T_0 is the temperature at which the diffusion of ions ceases to exist and may be considered as the glass transition temperature of polymer-gelled system. Accordingly, by using the polymer with lower T_g to gel the electrolyte system in order to decrease T_0, the conductivity should be increased. As a result, the fabricated DSSC should have more photocurrent and greater η.

Therefore, in the present work we have prepared poly(methyl acrylate) (PMA), poly(vinyl acetate) (PVAc) and poly(*n*-isopropyl acrylamide) (PNIPAAm) latices with their respective T_g of 6, 32, and 145 °C via soap-free emulsion polymerization, which were then employed to gel the LiI/I_2/tertiary butylpyridine (TBP) electrolyte solutions in acetonitrile and individually applied to fabricate the DSSCs based on the *cis*-di(thiocyanato)bis(2,2′-bipyridyl-4,4′-dicarboxylate)ruthenium(II) dye. Their photovoltaic properties such as photocurrent–voltage characteristics, incident monochromatic photon to current conversion efficiency (IPCE) and electrochemical impedance spectroscopy (EIS) were investigated. The results were then correlated with the measured molar conductivity of polymer-gelled electrolytes and the glass transition temperature of gelatinizing polymers.

2. Experimental

2.1. Materials

Methyl acrylate (MA), vinyl acetate (VAc), and *n*-isopropyl acrylamide (NIPAAm) monomers were from Acros. MA and VAc were distilled and NIPAAm was recrystallized before used. Potassium persulfate (KPS, Acros) was directly used as an initiator for soap-free emulsion polymerization. Anhydrous lithium iodide (LiI), iodine (I_2), poly(ethylene glycol) (PEG, molecular weight of 20,000) and 4-tertiary butyl pyridine (TBP) were obtained from Merck and titanium isopropoxide (TTIP, >98%) was from Acros and used as such. Acetonitrile and tertiary butanol were purchased from Merck. The *cis*-di(thiocyanato)bis(2,2′-bipyridyl-4,4′-dicarboxylate)ruthenium(II) dye was the commercial product by the trade name N3 obtained from Solaronix S.A., Aubonne, Switzerland.

PMA, PVAc and PNIPAAm latices were prepared by soap-free emulsion polymerization [26–28]. For preparation of PMA and PVAc latices, 9.5 g monomer was added into a three-neck flask, which has already been loaded with 125 mL deionized water and 0.3852 g KPS at room temperature. The solutions were then heated to 70 °C with stir and conducted polymerization overnight until no further polymerization was detected. The resulting latices were conglomerated by the addition of ethanol and then filtered, washed with de-ionized water three times, and dried at 60 °C for one day. For preparation of PNIPAAm latex, 2.26 g NIPAAm monomer was added to the solution of 100 ml deionized water and 0.11 g KPS. The solution was heated to 80 °C with stir for polymerization. After no further polymerization was detected (~3 h), the latex were immediately filtered, washed with deionized hot water (~80 °C) three times, and dried at 60 °C for one day. All the dried latices were ground into a powder form.

2.2. Preparation of polymer-gelled electrolytes

The electrolyte solution composed of proper amounts of LiI, I_2, and TBP in acetonitrile was prepared in dry box first. Then, the dried polymer powders of PMA, PVAc, and PNIPAAm were individually added to the electrolyte solution at the amount of 25 vol% of acetonitrile, which were then heated to 50 °C with sonication until the solutions were homogeneously gelled. The final concentrations of the polymer-gelled electrolytes were 0.5 M LiI, 0.05 M I_2 and 0.5 M TBP.

2.3. Preparation of TiO_2 electrode and fabrication of dye-sensitized Solar Cells

Gelled-type dye-sensitized solar cells were fabricated using FTO glass (20–25 Ω/□) as subtracts for both photoelectrode and counter-electrode [29]. The counter-electrodes were fabricated by depositing a thin Pt layer with sputtering. For preparation of photoelectrode, a mesoporous nano-structured film of anatase TiO_2 coated on the FTO glass subtracts was fabricated by sol–gel process according to the literature [5]. In general, 72 mL TTIP was added to 430 mL of 0.1 M HNO_3. After vigorously stirring for 30 min, the solution was heated to 85–90 °C and kept stirring for 8 h for peptization. After filtered to remove the large particles, the solution was reacted in the autoclave at 240 °C for 12 h. After cooled, it was concentrated to 13 wt% of TiO_2. PEG was then added to the solution in 30% of TiO_2 weight. After further stirring for 5 h to obtain the TiO_2 paste, it was deposited on the FTO glass subtract using a glass rod for spreading and an adhesive tape as a spacer to control the thickness to ~120 μm. The photoelectrode was obtained by heating the TiO_2 on the FTO glass in an oven at 450 °C for 30 min and repeating the coating and heating process two more times to complete the sintering process.

An active area of 0.25 cm^2 was selected from the sintered electrode, immersed in acetonitrile/teritiary butanol mixed solvent (volume ratio 1:1) containing 3×10^{-4} M *cis*-di(thiocyanato) bis(2,2′-bipyridyl-4,4′-dicarboxylate)ruthenium (II) for 24 h, rinsed with acetone and dried. Three polymer-gelled electrolytes were then individually applied on the dye-sensitized electrodes. However, in order to completely wet the electrodes, they were heated up to ~50 °C in advance to lower the viscosity. The thickness of all the polymer-gelled electrolytes was controlled to ~50 μm by the spacer. The assembly of gelled-type DSSCs was done by pressing the counter-electrode against the coated dye-sensitized electrode.

2.4. Characterization

Molecular weights of PMA, PVAc, and PNIPAAm were measured by gel permeation chromatography (GPC). The measurement was carried out at 40 °C with a Testhigh series III pump and a Testhigh ultraviolet (UV) detector model 500. One Phenol Gel 550A column and two Phenol Gel MXL columns in series were used with tetrahydrofuran as a mobile phase (1 mL/min). The molecular weights and molecular weight distributions were estimated by reference to the polystyrene standard. Glassy transition temperature was measured by using a differential scanning calorimeter (DSC, Perkin–Elmer Pyris 6) at a heating rate of 10 °C/min. The viscosity of individual polymer-gelled electrolytes was measured by using a Brookfield Model LVDV II viscometer. Their ionic conductivities after gradual dilution with acetonitrile were measured by using a Radiometer Copenhagen CDC-230 conductivity meter thermostated at 30 °C with a deviation of 0.01 °C [30,31]. UV/vis absorption spectrum of *cis*-di(thiocyanato)bis(2,2′-bipyridyl-4,4′-dicarboxylate)ruthenium (II) solution in acetonitrile/teritiary butanol mixed solvent was recorded on a Jasco model 555 spectrometer.

2.5. Photoelectrochemical measurements

The photoelectrochemical characterizations of the DSSCs were carried out using an AM 1.5 simulated light radiation. The light source was emitted from a 450 W Xe lamp (Oriel, #6266) equipped with a water-based IR filter and AM 1.5 filter (Oriel, #81075). The open-circuit voltages (V_{oc}) and photocurrent–voltage curves were recorded with a potentiostat/galvanostat (PGSTAT 30, Autolab, Eco-Chemie, Netherland). For the IPCE measurement, light from a 450 W xenon lamp was focused through a Triax-180 double monochromator (Jobin Yvon Ltd., UK) onto the photovoltaic cell under test. The monochromator was scanned through the UV/vis spectrum to generate the IPCE as defined IPCE $= 1240(J_{sc}/\lambda_w)$, where λ is the wavelength, J_{sc} is the short-circuit current (mA/cm^2), and w is the incident irradiative flux (W/m^2).

AC impedance measurements were performed with the above-mentioned potentiostat/galvanostat equipped with FRA2 module under constant light illumination of 100 mW/cm^2. The frequency range explored was 65 kHz to 10 mHz. The applied bias voltage and ac amplitude were set at open-circuit voltage of the DSSCs and 10 mV, respectively between the counter-electrode and the photoelectrode, starting from the short-circuit condition [14,32].

3. Results and discussion

3.1. Glass transition temperature and ionic conductivity

Fig. 1 shows the DSC thermograms of PMA, PVAc and PNIPAAm polymers measured at a scanning rate of 10 °C/min. Their T_g estimated from the step change of the curves were listed in Table 1 along with the measured number average molecular weights and polydispersity indexes (PDI). All three polymers are vinyl polymers but carry different side groups. PMA is isomeric with PVAc but its T_g is much lower owing to the fact that hindrance to rotation offered by the ester side groups in the acrylate is less than in the acetate [33]. PNIPAAm has the highest T_g owing to the hydrogen bonding provided by the *n*-isopropyl acrylamide side groups. As PMA, PVAc and PNIPAAm polymers were employed to gel the 0.5 M LiI/0.05 M I_2/0.5 M TBP electrolyte system in acetonitrile, the viscosity was increased to 3630, 2360, and 800 poise, respectively. On the contrary, because the polymers were plasticized by acetonitrile, their glass transition temperature was significantly decreased according to the Kelly and Bueche equation [34].

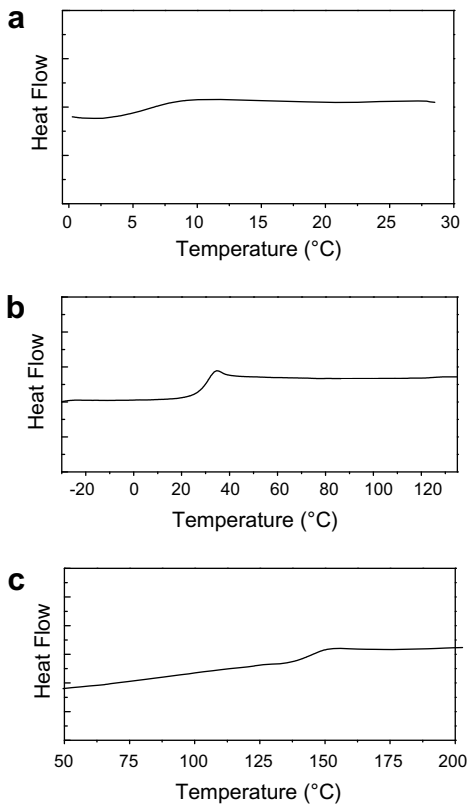

Fig. 1. DSC thermograms of: (a) PMA, (b) PVAc, and (c) PNIPAAm.

Table 1
Properties of polymers

	Mn × 10^4	PDI	T_g (°C)
PMA	8.78	1.84	6
PVAc	30.37	2.14	32
PNIPAAm	30.28	2.13	145

$$T_g = \frac{v_p T_{g,p}(\alpha_l - \alpha_g) + v_d T_{g,d}\alpha_d}{v_p(\alpha_l - \alpha_g) + v_d\alpha_d} \quad (4)$$

where $T_{g,p}$ and $T_{g,d}$ are the glass transition temperature of polymers and acetonitrile, v_p and v_d are the volume fractions of polymers and acetonitrile, $\alpha_l - \alpha_g$ is the difference between thermal expansion coefficients of liquid state and glassy state of polymers, and α_d is the thermal expansion coefficient of acetonitrile. If 49 °K is adopted as the T_g

of acetonitrile [35], and $\alpha_l - \alpha_g = 4.8 \times 10^{-4}\ ^\circ K^{-1}$ and $\alpha_d = 1.0 \times 10^{-3}\ ^\circ K^{-1}$ were adopted [33], T_g of the PMA-gelled, PVAc-gelled and PNIPAAm-gelled systems can be estimated as 80.7, 84.3, and 99.9 °K, respectively on the basis of Eq. (4).

Because the viscosity of polymer-gelled electrolytes was too high for the measurement of ionic conductivity, they were diluted by acetonitrile. Since only LiI is a strong electrolyte, its concentration after dilution was used as a parameter to estimate the molar conductivity and the results with respect to the square root of concentration were plotted in Fig. 2. According to Kohlrausch's law for the molar conductivity of strong electrolytes [36]

$$\Lambda = \Lambda^0 - \kappa\sqrt{c} \tag{5}$$

where Λ^0 is the limiting molar conductivity, c is the concentration, and κ is a constant. Thus, the limiting molar conductivities and molar conductivities at 0.5 M LiI for all three polymer-gelled electrolyte systems can be estimated by Eq. (5). The molar conductivity of LiI at 0.5 M was then converted into the ionic conductivity by $\sigma = \Lambda \times c$. The results were listed in Table 2, indicating that the polymer-gelled electrolyte system with higher T_g has lower ionic conductivity, which can be justified by the VFT equation as shown in Eq. (3).

3.2. Photocurrent–voltage characteristics

Fig. 3 shows the photocurrent–voltage characterization plots of the DSSCs gelled with PMA, PVac, and PNIPAAm, respectively. Their J_{sc}, V_{oc}, η, and fill factor were summarized in Table 3. It is amazing

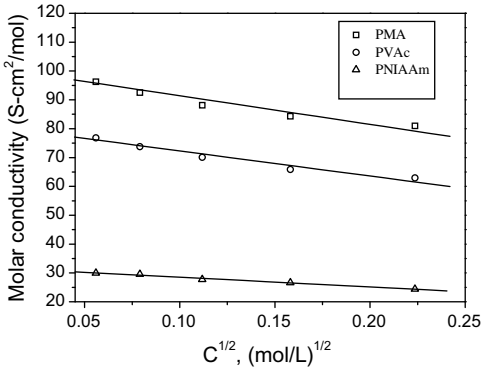

Fig. 2. Molar conductivities as a function of the square root of LiI concentration after gradual dilution with acetonitrile for the (□) PMA-gelled, (○) PVAc-gelled, and (Δ) PNIPAAm-gelled 0.5 M LiI/0.05 M I_2/0.5 M TBP electrolyte systems.

Table 2
Estimated conductivity data of polymer-gelled LiI/I_2/TBP electrolytes in acetonitrile

	Λ^0 (S cm^2/mol)	Λ (S cm^2/mol) at 0.5 M LiI at 0.5 M LiI	σ (mS/cm) at 0.5 M LiI
PMA	101.34	51.73	25.87
PVAc	80.97	37.54	18.77
PNIPAAm	32.25	6.72	3.36

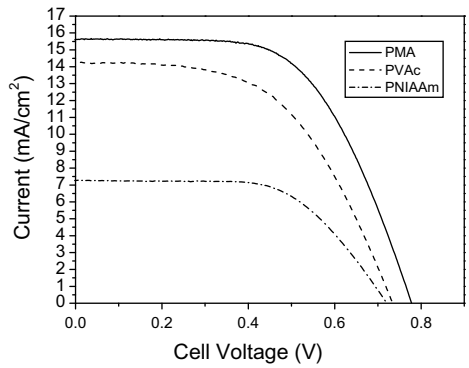

Fig. 3. Photocurrent-voltage characterization plots of the DSSCs with (—) PMA-gelled, (–) PVAc-gelled, and (- -) PNIPAAm-gelled 0.5 M LiI/0.05 M I_2/0.5 M TBP electrolyte systems under AM 1.5 and 100 mW/cm^2 illumination.

to find that all the J_{sc}, V_{oc} and η were increased with decreasing the T_g of gelatinizing polymers. Especially, the DSSCs gelled with PMA has η = 7.17%, next to the highest 7.72% even reported in the literature for the polymer-gelled DSSC [37]. The polymer-gelled electrolyte systems that provided higher photocurrent for the DSSC also showed higher ionic conductivity, which can be justified by Eqs. (1) and (2). In brief, the diffusion coefficient of oxidized redox couples is greater with higher ionic conductivity, leading to the increase of photocurrent.

Fig. 4 shows the IPCE spectra of the DSSCs gelled with PMA, PVAc, and PNIPAAm, respectively. The UV/vis absorption spectrum of *cis*-di(thiocyanato)-bis(2,2′-bipyridyl-4,4′-dicarboxylate)ruthenium (II) in solution was also included for comparison. Although the DSSCs with higher power efficiency have greater IPCE, all of the IPCE spectra have roughly similar pattern as the UV/vis absorption spectrum of the dye.

3.3. Electrochemical impedance spectroscopy analysis

The electrochemical impedance spectroscopy (EIS) technique has been used to characterize the

Table 3
Photovoltaic characteristics and EIS impedance data of DSSCs gelled with different polymers

	V_{oc} (V)	J_{sc} (mA/cm^2)	η (%)	Fill factor	R_s (Ω)	R_1 (Ω)	R_2 (Ω)	R_3 (Ω)
PMA	0.78	15.64	7.17	0.59	23.19	7.79	18.6	12.64
PVAc	0.73	14.28	5.62	0.54	27.28	7.56	11.65	13.98
PNIPAAm	0.72	7.28	3.17	0.60	39.05	10.1	29.43	59.15

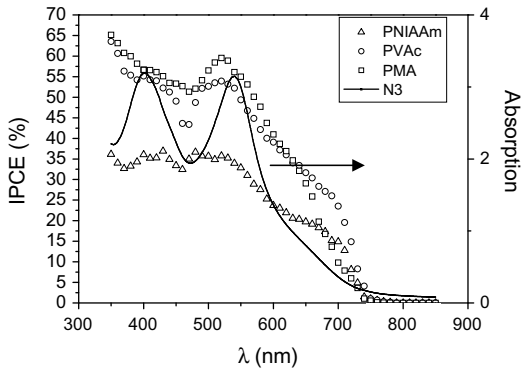

Fig. 4. IPCE spectra of the DSSCs with (□) PMA-gelled, (○) PVAc-gelled, and (Δ) PNIPAAm-gelled 0.5 M LiI/0.05 M I_2/0.5 M TBP electrolyte systems. UV/vis absorption spectrum of N3 dye in acetonitrile/teritiary butanol mixed solvent included for comparison (see right axis).

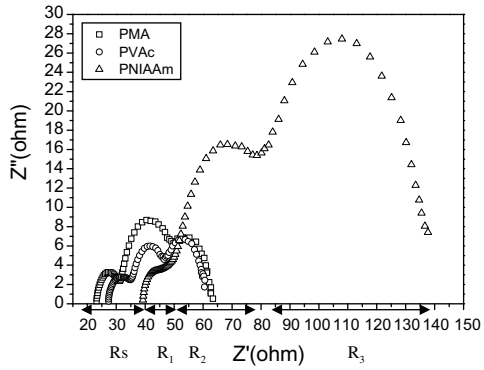

Fig. 5. Electrochemical impedance spectra of the DSSCs with (□) PMA-gelled, (○) PVAc-gelled, and (Δ) PNIPAAm-gelled 0.5 M LiI/0.05 M I_2/0.5 M TBP electrolyte systems under open-circuit condition and 100 mW/cm^2 illumination. The double-ended arrows indicated the approxmate ranges of R_s, R_1, R_2 and R_3 for the PNIPAAm-gelled DSSC.

kinetics of the DSSCs by analyzing the variation in impedances associated with the different configurations [38–40]. In this work, the analysis was mainly aimed at the Nyquist plots for the DSSCs gelled with PMA, PVAc and PNIPAAm, respectively under open-circuit voltage and 100 mW/cm^2 illumination. All the impedance spectra shown in Fig. 5 illustrated three semicircles in the measured frequency range of 65 kHz–10 mHz. Notably, R_s, the ohmic serial resistance, is associated with the series resistance of the electrolytes and electric contacts in the DSSCs [29]. R_1, the charge transfer resistance, occurs at the Pt counter-electrode. R_2 has been associated with the resistance at the TiO_2/dye/electrolyte interface, whereas R_3 has been associated with the Nernstian diffusion within the electrolytes [39]. All the measured impedance data for the polymer-gelled DSSCs are also included in Table 3. Apparently, the DSSC gelled with PNIPAAm has the highest resistances in the current path across the device. Besides, the trend of changes for R_s and R_3 with different gelatinizing polymers follows the similar trend of ionic conductivities and photocurrents. Notably, the substantial reduction of power efficiency for PVAc-gelled DSSC compared to the PMA-gelled one was also related to its lower V_{oc} (see Table 3). After all, it can be certain that using the polymer with lower T_g to gel the electrolyte system plays a decisive role to enhance the photocurrent and powder efficiency of DSSC.

4. Conclusions

PMA, PVAc, and PNIPAAm latices fabricated by soap-free emulsion polymerization were employed to gel the 0.5 M LiI/0.05 M I_2/0.5 M TBP electrolytes in acetonitrile for preparation of the gelled-type DSSCs. Photocurrent, power efficiency and IPCE of the DSSCs were increased as the polymer of lower T_g was used to gel the electrolytes, owing to the fact that it contributes to the increase of ionic conductivity as predicted by the VFT equation. The electrochemical impedance spectroscopy of polymer-gelled DSSCs also indicated less resistance associated with the Nernstian diffusion within the electrolytes as the polymer of lower T_g was adopted. Notably, the power efficiency of PMA-gelled DSSC can reach 7.17%, next to the highest value ever reported in the literature.

Acknowledgements

The authors would like to acknowledge the financial support of the National Science Council in Taiwan, Republic of China, through Grant NSC 95-2221-E-002-MY3.

References

[1] O'Regan B, Grätzel M. Nature 1991;353:737S.
[2] Hara K, Sato T, Katoh R, Furube A, Ohga Y, Shinpo A, et al. J Phys Chem B 2003;107:597.
[3] Ferrere S, Gregg BA. J Phys Chem B 2001;105:7602.
[4] Grätzel M. J Photochem Photobiol A 2004;164:3.
[5] Barbé CJ, Arendse F, Comte P, Jirousek M, Lenzmann F, Shklover V, et al. J Am Ceram Soc 1997;80:3157.
[6] Nogueira AF, Durrant JR, De Paoli MA. Adv Mater 2001;13:826.
[7] Stergiopoulos T, Arabatzis IM, Katsaros G, Falaras P. Nano Lett 2002;2:1259.
[8] Katsaros G, Stergiopoulos T, Arabatzis IM, Papadokostaki KG, Falaras P. J Photochem Photobiol A: Chem 2002;149:191.
[9] O'Regan B, Schwartz DT. Chem Mater 1995;7:1349.
[10] Nogueira AF, De Paoli MA. Sol Energ Mater Sol Cells 2000;61:135.
[11] Ren Y, Zhang Z, Gao E, Fang S, Cai S. J Appl Electrochem 2001;31:445.
[12] De Paoli MA, Nogueira AF, Machado DA, Longo C. Electrochim Acta 2001;46:4243.
[13] Stathatos E, Lianos P. Int J Photoenerg 2002;4:11.
[14] Longo C, Freitas J, De Paoli MA. J Photochem Photobiol A: Chem 2003;159:33.
[15] Wu J, Lan Z, Wang D, Hao S, Lin J, Wei Y, et al. J Photochem Photobiol A: Chem 2006;181:333.
[16] Ren Y, Zhang Y, Fang S, Yang M, Cai S. Sol Energ Mater Sol Cells 2002;71:253.
[17] Kang MS, Kim JH, Kim YJ, Won J, Park NG, Kang YS. Chem Commun 2005:889.
[18] Li W, Kang J, Li X, Fang S, Lin Y, Wang G, et al. J Photochem Photobiol A: Chem 2005;170:1.
[19] Kim MR, Jin SH, Park SH, Lee HJ, Kang EH, Lee JK. Mol Cryst Liquid Cryst 2006;444:236.
[20] Kang MG, Kim KM, Ryu KS, Chang SH, Park NG, Hong JS, et al. J Electrochem Soc 2004;151:E257.
[21] Kaneko M, Hoshi T, Kaburagi Y, Ueno H. J Electroanal Chem 2004;572:21.
[22] Tu CW, Liu KY, Chien AT, Yen MH, Weng TH, Ho KC, et al. J Polym Sci Part A: Polym Chem 2008;46:47.
[23] Wang P, Zakeeruddin SM, Moser JE, Nazeeruddin MK, Sekiguch T, Grätzel M. Nat Mater 2003;2:402.
[24] Huang SY, Schlichthörl G, Nozik AJ, Grätzel M, Fank AJ. J Phys Chem B 1997;101:2576.
[25] Gu GY, Bouvier S, Wu C, Laura R, Rzeznik M, Abraham KM. Electrochim Acta 2000;45:3127.
[26] Lin KF, Shieh YD. J Appl Polym Sci 1998;69:2069.
[27] Lin KF, Shieh YD. J Appl Polym Sci 1998;70:2313.
[28] Chien AT, Lin KF. J Polym Sci Part A: Polym Chem 2007;45:5583.
[29] Longo C, Nogueira AF, De Paoli MA, Cachet H. J Phys Chem B 2002;106:5925.
[30] Lin KF, Young SL, Cheng HL, Cheng YH. Macromolecules 1999;32:4602.
[31] Lin KF, Cheng HL, Cheng YH. Polymer 2004;45:2387.
[32] Bernard MC, Cachet H, Falaras P, Hugot-Le Goff A, Kalbac M, Lukes I, et al. J Electrochem Soc 2003;150:E155.
[33] Meares P. Polymers: structure and bulk properties. Princeton: Van Nostrand; 1964.
[34] Kelley FN, Bueche F. J Polym Sci 1961:549.
[35] Ghoral PK, Matyushov DV. J Chem Phys 2006;124:144510.
[36] Atkins PW. Physical Chemistry. 5th ed. Oxford: Oxford University Press; 1994.
[37] Wang L, Fang S, Lin Y, Zhou X, Li M. Chem Commun 2005:5687.
[38] Kern R, Sastrawan R, Ferber J, Stangl R, Luther J. Electrochim Acta 2002;47:4213.
[39] Han L, Koide N, Chiba Y, Mitate T. Appl Phys Lett 2004;84:2433.
[40] Kron G, Egerter T, Nelles G, Yasuda A, Werner JH, Rau U. Thin Solid Film 2002;403:242.